J Wood Sci (2011) 57:189–194
DOI 10.1007/s10086-010-1160-z

ORIGINAL ARTICLE

Soichi Tanaka · Yuko Fujiwara · Yoshihisa Fujii
Shogo Okumura · Hiroyoshi Togo · Naoya Kukutsu
Tadao Nagatsuma

Effect of grain direction on transmittance of 100-GHz millimeter wave for hinoki (*Chamaecyparis obtusa*)

Received: May 26, 2010 / Accepted: October 13, 2010 / Published online: February 26, 2011

Abstract The attenuation coefficients of 100-GHz millimeter waves polarized linearly were measured for cross-cut, quarter-sawn, and flat-sawn boards of hinoki (*Chamaecyparis obtusa*) that were 0.2–2.0 cm thick. This was done to examine the applicability of free-wave propagation theory for applying electromagnetic waves to wood. It was found that the transmittance of a millimeter wave through the specimen boards was lower when the fiber direction of a board was parallel to the direction of the electric field of the incident wave than when the fiber direction was perpendicular to the electric field, and there was little difference in the transmittance between the tangential and radial directions for the former case. These findings can be quantitatively explained by using propagation theory and the dielectric properties of wood.

Key words Millimeter wave · Transmittance · Attenuation · Fiber direction · Anisotropy

Introduction

The millimeter-wave technique, in which electromagnetic waves in the frequency range 30–300 GHz are used, has only recently been developed and is expected to be used not only for communications but also for imaging in dielectric materials.[1–5] The millimeter-wave imaging technique can be used in the nondestructive testing of wood, and it has a higher resolution than the microwave technique which is also used for the nondestructive evaluation of wood. However, there have been only a few basic studies[6,7] on the dielectric properties of wood in the millimeter wave frequency range. These dielectric properties are generally characterized by their parameters such as their complex permittivity or attenuation and phase coefficients. To explain the dielectric property of orthotropic materials such as wood, these parameters need to be known in three directions along the principal axes of the anisotropy.

In previous studies,[8–11] the dielectric properties of wood have been measured by using methods in the microwave frequency range below 30 GHz, i.e., detection of microwaves transmitted through waveguides filled with wood[8,9] and detection of free microwave beams transmitted through and reflected in wood.[10,11]

The former method is better than the latter in terms of accuracy when measuring the permittivity because the electric field is more stable in and around the specimen in the waveguide, and the free electric field used in the latter method is often unstable because of scattering and diffraction of the microwave induced by components of the apparatus, especially in the microwave frequency range. The latter method is preferable for the nondestructive evaluation of wood, especially when using two- or three-dimensional imaging, because the local permittivity in wood can be measured using the latter method, while only the average permittivity of the whole specimen is obtained by the former method. In the millimeter wave frequency range, it is difficult to evaluate the dielectric properties of wood using the former method since a cross section of the waveguide, which is usually only a few millimeters square, is too small to ignore the effect of the heterogeneity of the wood, such as the annual ring structure. The latter method is, therefore, required to obtain a more accurate evaluation of the dielectric properties of wood in the millimeter frequency range.

There have been two previous studies on the measurement of the dielectric properties of wood in the frequency ranges that include millimeter waves. Reid and Fedosejevs[6]

S. Tanaka (✉) · Y. Fujiwara · Y. Fujii · S. Okumura
Graduate School of Agriculture, Kyoto University,
Kitashirakawaoiwake-cho, Sakyo-ku, Kyoto 606-8502, Japan
Tel. +81-75-753-6245; Fax +81-75-753-6245
e-mail: stanaka@h3news1.kais.kyoto-u.ac.jp

H. Togo · N. Kukutsu
NTT Microsystem Integration Laboratories, Atsugi 243-0198, Japan

T. Nagatsuma
Graduate School of Engineering Science, Osaka University,
Toyonaka 560-8531, Japan

Part of this report was presented at the Annual Meeting of the Japan Wood Research Society, Tsukuba, March 2008

measured the dielectric properties of air-dried spruce in the frequency range 100–1600 GHz by using a terahertz pulse wave. Oyama et al.[7] measured the dependence of the dielectric properties of wood on its density and moisture content; however, they did not discuss the anisotropy of the dielectric properties of the wood.

For the anisotropy of the dielectric properties of wood, Torgovnikov[12] suggested that the difference in dielectric properties of wood between the radial and tangential directions decreases with an increase in frequency above the microwave frequency range. This has, however, not been verified through experimentation.

In this article, the attenuation and phase coefficients of hinoki (Japanese cypress) in the longitudinal, radial, and tangential directions for quarter-sawn, flat-sawn, and crosscut boards were evaluated while taking into account the effect of the anisotropy of the wood on its dielectric properties. A 100-GHz free electromagnetic wave, which is a representative frequency of the millimeter wave range, was used on the basis of the behavior of the electromagnetic wave in wood as an orthotropic material. Furthermore, the dependency of the transmittance of the millimeter wave through hinoki in the grain direction was discussed by using propagation theory with the attenuation and phase coefficients in order to examine the applicability of the propagation theory to wood.

Theory

Wood is generally orthotropic in permittivity, and the three principal axes of the anisotropy are the fiber direction (L), the radial direction (R), and the tangential direction (T). These three directions can be used to explain the permittivity of wood in an arbitrary direction. Let the principal axes of anisotropy correspond to the three rectangular coordinate axes (X, Y, Z) that describe a rectangular parallelepiped specimen. A millimeter wave is treated as a free electromagnetic wave that transmits in the z direction and that is polarized linearly in the x direction. The relationship between the coordinate axes for the electromagnetic wave and the specimen is shown in Fig. 1. By letting the z-axis be parallel to the Z-axis, the angle between the x- and X-axes, θ, is equal to that between the y- and Y-axes. Let the thickness of the specimen be d and the electric fields before and after the penetration through the specimen be E_0 and E, respectively. If the heterogeneity of a wood specimen is such as the annual ring structure can be ignored, the transmittance, P, can be formulated as follows:[6]

$$P = \frac{|E|}{|E_0|} = t' \exp\left(-\frac{1}{2}\alpha_X d\right) \left|\cos^2\theta + \exp\left\{\frac{1}{2}(\alpha_X - \alpha_Y)d\right\}\exp\{j(\beta_X - \beta_Y)d\}\sin^2\theta\right|, \quad (1)$$

where α_X, α_Y, β_X, and β_Y are the attenuation and the phase coefficients in the X and Y directions, respectively; t' is the product of the Fresnel transmission coefficients of the wood-to-air and air-to-wood interfaces and is regarded as a constant, although it depends on θ. If x is parallel or perpendicular to X, i.e., θ is 0° or 90°, Eq. 1 can be rewritten as follows:

$$P_X = t' \exp\left(-\frac{1}{2}\alpha_X d\right) (\theta = 0°) \text{ or} \quad (2)$$

$$P_Y = t' \exp\left(-\frac{1}{2}\alpha_Y d\right) (\theta = 90°), \quad (3)$$

where P_X and P_Y are the transmittances in the X and Y directions, respectively. These equations imply that the dependences of P on d in the X and Y directions are affected by the attenuation coefficients in the X and Y directions, respectively.

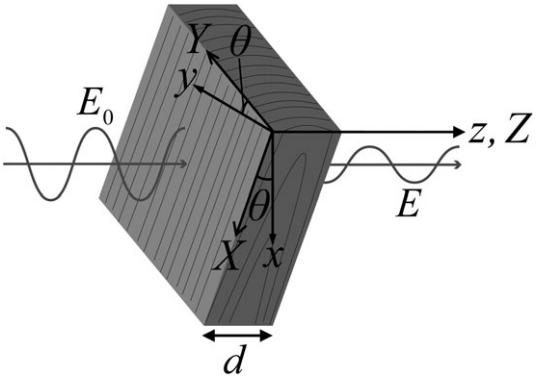

Fig. 1. Relation between coordinate axes (X, Y, Z) of specimen and coordinate axes (x, y, z) of propagation of electromagnetic waves for quarter-sawn boards. The axes X and Y are parallel to the longitudinal (L) and radial (R) directions, respectively

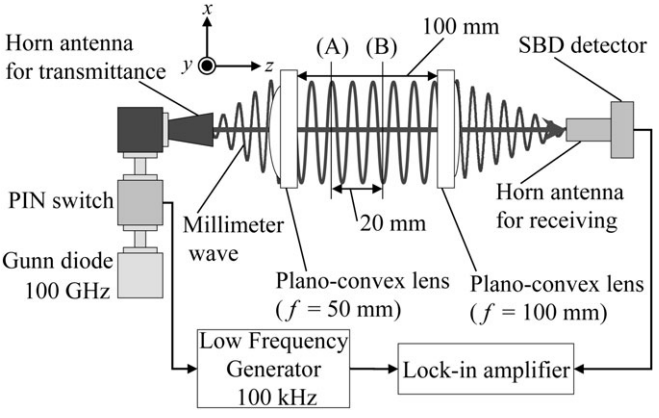

Fig. 2. Experimental setup for generation and detection of millimeter waves arranged in coordinate system (x, y, z). *SBD*, Schottky barrier diode. *A*, and *B* are reference planes

Experimental

Apparatuses

The setup for the millimeter wave transmitter and receiver system arranged in coordinate system (x, y, z) is shown in Fig. 2. A Gunn diode was used to generate the millimeter

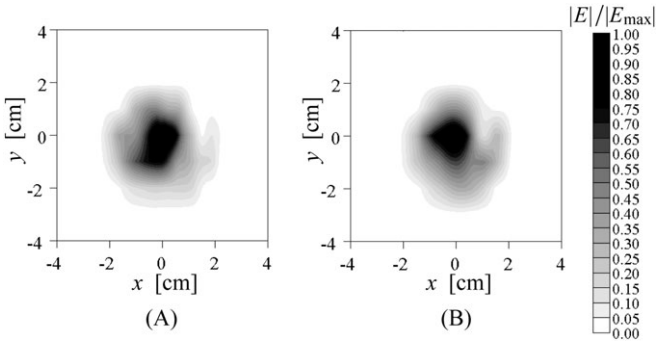

Fig. 3. Distribution of relative beam magnitude on *xy* plane at positions (A) and (B) in Fig. 2. The relative magnitude is the ratio of the *x* element of the electric field at a given point to that at the point where the maximum electric field appears

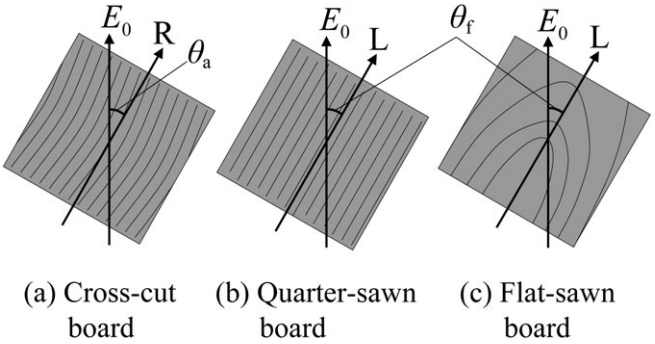

Fig. 4a–c. Relation between electric field direction, E_0, and principal axes of wood, L, R, and tangential (T), in coordinate system (x, y, z). **a** Cross-cut board, **b** quarter-sawn board, **c** flat-sawn board. θ_a, annual ring deviation angle; θ_f, fiber deviation angle

wave at an average output power of 10 mW at 100 GHz. The output signal from the diode was modulated by a PIN-diode. A millimeter wave polarized linearly in the *x* direction was radiated in the *z* direction from a horn antenna and was transformed into a parallel beam using a Teflon plano-convex lens, 50 mm in diameter, with a focal length of 50 mm. The beam was focused onto a sensor with another plano-convex lens, 50 mm in diameter, with a focal length of 100 mm. The sensor received the electric field component parallel to the *x* direction. The received wave signal was processed in a lock-in amplifier (Stanford Research Systems model SR850 DSP). The magnitude of the electric field of the millimeter wave was obtained as a voltage at the lock-in amplifier. The positions and the directions of the lenses in Fig. 2 were determined so that the gain of the millimeter wave was maximized.

The distribution of the relative magnitude of the beam on the *xy* plane at positions (A) and (B) between the two plano-convex lenses (Fig. 2) is shown in Fig. 3. This distribution was obtained by scanning with the sensor mentioned above on the *xy* planes at positions (A) and (B). Figure 3 shows that there is no significant difference in the distribution of the beam amplitude between (A) and (B) and that a specimen set between (A) and (B) is irradiated with millimeter waves over an area 40 mm in diameter. It was confirmed that the distributions obtained at positions other than (A) and (B) were almost the same as those in Fig. 3.

The transmittance of millimeter waves was measured for wood specimens that were set between (A) and (B) in such a manner that their major faces were perpendicular to the beam. The transmittance P was estimated according to the right side of Eq. 1.

Specimens

Cross-cut (TR, parallel to TR plane), quarter-sawn (LR), and flat-sawn (LT) boards at nominal thicknesses of 0.2, 0.3, 0.5, 0.9, 1.5, and 2.0 cm were prepared from hinoki heartwood (Japanese cypress, *Chamaecyparis obtusa*) under air-dry conditions (MC = 8%). The quarter- and flat-sawn boards were cut from a piece of lumber with an average air-dry density of 347 kg/m^3, and the cross-cut boards were cut from another piece of lumber with an average air-dry density of 383 kg/m^3. Clear hinoki boards were used because they are straight-grained, show small differences in density between early- and latewood, and adequately satisfy the assumption that any heterogeneity of the specimen, e.g., the annual ring structure, can be ignored.

As shown in Fig. 4, the annual ring deviation angle, θ_a, is defined as the angle between the tangential direction of the wood specimen and the direction of the electric field of the incident wave (*x* direction) for cross-cut boards, and the fiber deviation angle, θ_f, as the angle between the fiber direction and the *x* direction for quarter- and flat-sawn boards.

The principal axes X, Y, and Z (or z) of the anisotropy and the angle θ of the specimen mentioned in the Theory section correspond to T, R, L, and θ_a for cross-cut boards; L, R, T, and θ_f for quarter-sawn boards; and L, T, R, and θ_f for flat-sawn boards, respectively.

Measurement of transmittance

To examine the validity of the attenuation properties given by Eqs. 2 and 3, the transmittance P for each board of different thickness d was measured at $\theta = 0°$ and 180° and at $\theta = 90°$ and 270°, for cross-cut, quarter-sawn, and flat-sawn boards. Furthermore, to examine the validity of the anisotropy given by Eq. 1, the transmittance P was measured at intervals of 15° of the fiber deviation angle θ_f or the annual ring deviation angle θ_a from 0° to 360°.

Results and Discussion

Estimation of attenuation coefficient

Figures 5–7 show the relations between the transmittance P and the thickness of specimen d for cross-cut, quarter-sawn, and flat-sawn boards, respectively. In these figures, $\ln(1/P^2)$ shows a good linear relationship to d for all boards, which is consistent with the theory shown as Eqs. 2 and 3. Some irregularities in Figs. 5–7 could be due to the formation of

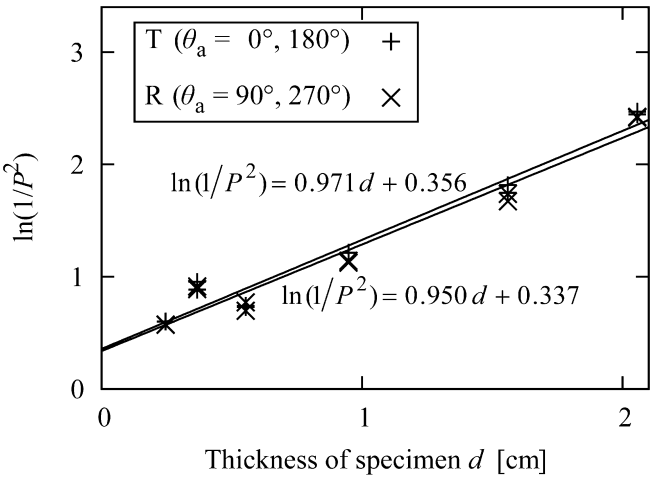

Fig. 5. Relation between thickness of specimen d and $\ln(1/P^2)$ in T and R directions for cross-cut boards. P, transmittance of millimeter wave. Coefficient of determination values, R^2, were 0.963 and 0.956 for the T and R directions, respectively

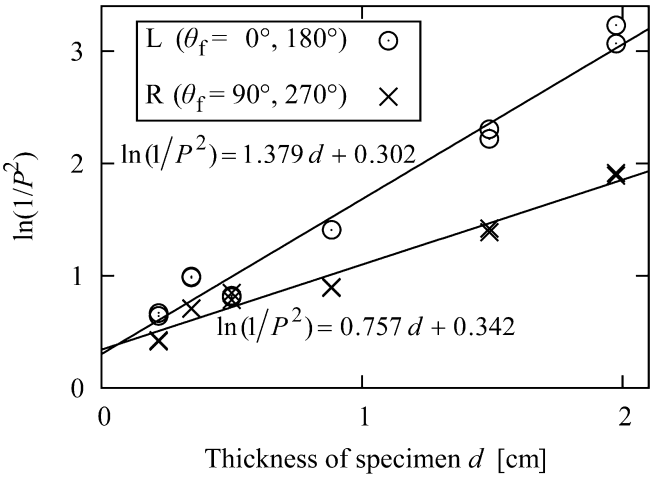

Fig. 6. Relation between thickness of specimen d and $\ln(1/P^2)$ in the L and R directions for quarter-sawn boards. R^2 values were 0.974 and 0.965 for the L and R directions, respectively

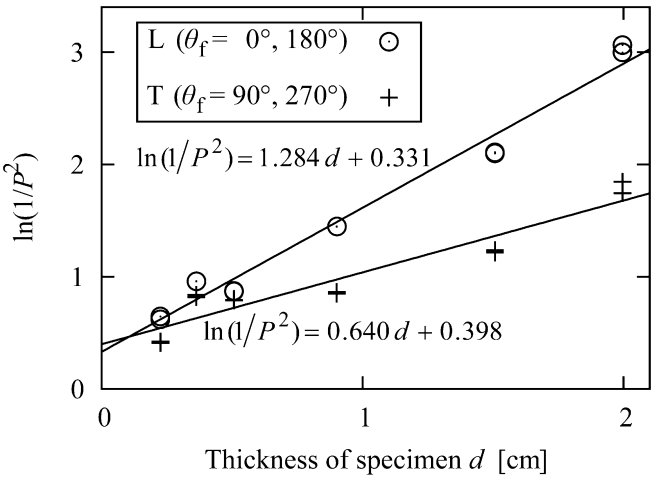

Fig. 7. Relation between thickness of specimen d and $\ln(1/P^2)$ in L and T directions for flat-sawn boards. R^2 values were 0.979 and 0.902 for the L and T directions, respectively

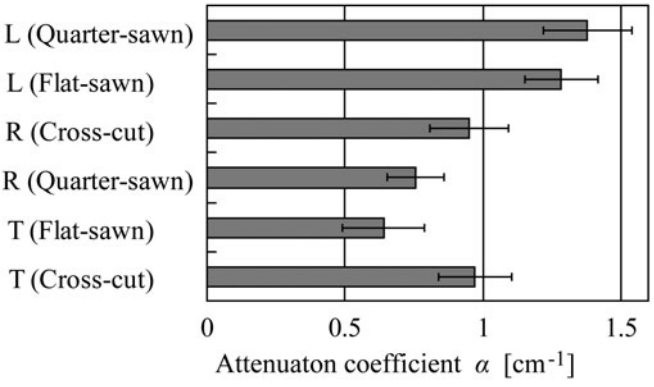

Fig. 8. Attenuation coefficients for each principal axis of anisotropy for quarter-sawn, flat-sawn, and cross-cut boards

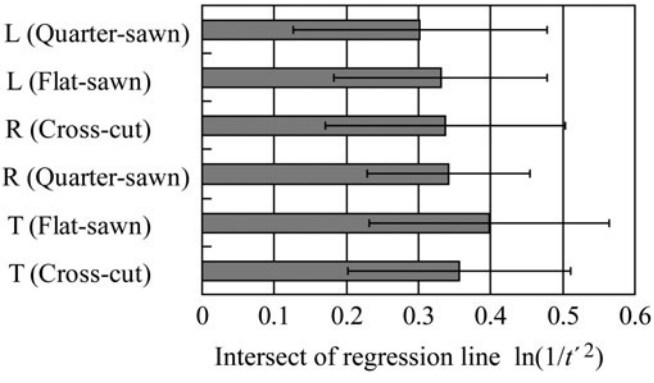

Fig. 9. Intercepts of regression lines for each principal axis of anisotropy for quarter-sawn, flat-sawn, and cross-cut boards. t' is the product of the Fresnel transmission coefficients of the wood-to-air and air-to-wood interfaces

a standing wave that results from interference between the incident and reflected waves, probably including the components of multiple reflections. The fact that the lines in Figs. 5–7 do not pass through the origin could be also due to the reflections. The slopes and intercepts of the regression lines in Figs. 5–7 were used to obtain the values of α and $\ln(1/t'^2)$ for each principal axis of the anisotropy, respectively (Figs. 8, 9). Figure 8 shows that there is little difference in α_L between the quarter- and flat-sawn boards and that α_R and α_T are almost identical and smaller than α_L. The values of α_R and α_T for cross-cut boards are almost identical and are larger than those for the quarter- and flat-sawn boards. This is probably because the average air-dry density of cross-cut boards was larger than that of quarter- and flat-sawn boards. These findings support Torgovnikov's prediction[12] that the dielectric properties of wood in the radial and tangential directions would be identical above the microwave frequency range.

The ordinate intercepts of the regression lines, $\ln(1/t'^2)$, were almost the same for all boards and were without any

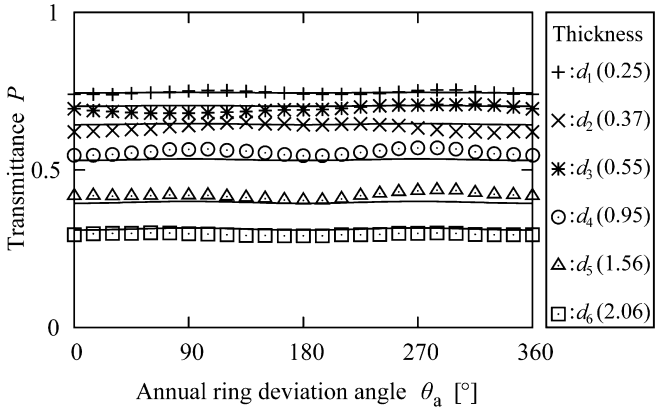

Fig. 10. Relation between θ_a and P for cross-cut boards with thicknesses of d_1 to d_6. *Numerals in parentheses* refer to measured board thicknesses in centimeters. The *solid curves* are drawn according to Eq. 1

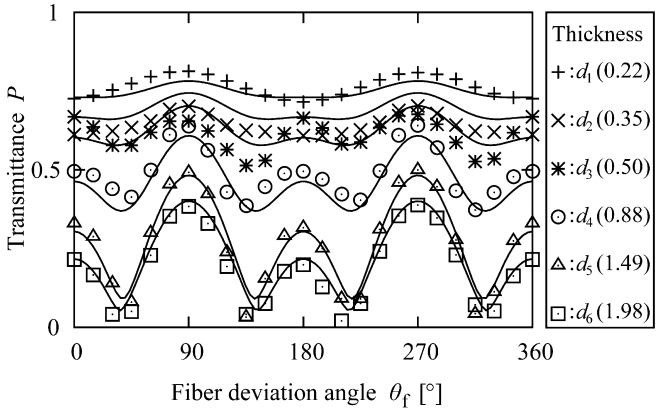

Fig. 11. Relation between θ_f and P for quarter-sawn boards with thicknesses of d_1 to d_6. *Numerals in parentheses* refer to measured board thicknesses in cm. The *solid curves* are drawn according to Eq. 1

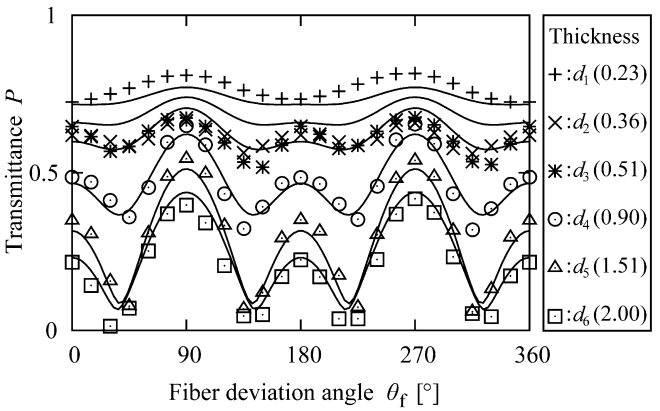

Fig. 12. Relation between θ_f and P for flat-sawn boards with thicknesses of d_1 to d_6. *Numerals in parentheses* refer to measured board thicknesses in cm. The *solid curves* are drawn according to Eq. 1

significant differences (Fig. 9). This implies that the Fresnel transmission coefficient is little affected by the fiber direction, namely that the influence of the anisotropy of wood on the behavior of the electromagnetic wave is markedly larger in the specimen than at the boundary between the specimen and the air. It is, however, not worth evaluating the absolute value t', since t' is affected by the components of multiple reflections, a phenomenon in which the millimeter wave reflects repetitively in a horn antenna to be used for the radiation and reception of the wave.

Dependency of transmittance on fiber direction and estimation of phase coefficient

Figures 10–12 show the experimental and theoretical relations of the transmittance P to the annual ring deviation angle θ_a for cross-cut boards and to the fiber deviation angle θ_f for quarter- and flat-sawn boards. The theoretical relations for each board were obtained by substituting the parameters from Figs. 8 and 9 into Eq. 1. The difference between two phase coefficients, $\Delta\beta = \beta_X - \beta_Y$, was estimated as the value that minimizes the sum of the squares of the differences between the theoretical (P) and experimental (P') transmittances, $J(\Delta\beta)$ in Eq. 4, for cross-cut, quarter-sawn, and flat-sawn boards:

$$J(\Delta\beta) = \sum_i \sum_j \left| P'(d_i, \theta_j) - P(d_i, \theta_j, \Delta\beta) \right|^2 \quad (4)$$

where d_i ($i = 1, 2, \ldots, 6$) are the specimen thicknesses shown in Figs. 10–12, and θ_j ($j = 1, 2, \ldots, 25$) are the fiber or annual ring deviation angles from 0° to 360° at intervals of 15°. To estimate $\Delta\beta$, which is a periodic function, from Eq. 4, $\Delta\beta$ was supposed to be in the range 0–10 rad/cm, since Reid and Fedosejevs[6] reported a value of 1.5 rad/cm for air-dry spruce at 100 GHz using a terahertz pulse wave. The estimated values of $\Delta\beta$ and the corresponding values of $J(\Delta\beta)$ are listed in Table 1. This table shows that the dielectric properties in the T and R directions are the same and are different from those in the L direction. This is consistent with the findings for the attenuation coefficient α shown in Fig. 8 and with Torgovnikov's predictions.

Table 1. Values for $\Delta\beta$ and $J(\Delta\beta)$ obtained for cross-cut, quarter-sawn, and flat-sawn boards

(X, Y)	$\Delta\beta = \beta_x - \beta_y$ (cm/rad)	$J(\Delta\beta)$
(T, R) Cross-cut	0.00	0.217
(L, R) Quarter-sawn	1.78	0.211
(L, T) Flat-sawn	1.79	0.302

$\Delta\beta$, difference between the two phase coefficients β_X and β_Y; $J(\Delta\beta)$, sum of the squares of the differences between the theoretical and experimental transmittances; L, the fiber direction; R, the radial direction; T, the tangential direction

In Figs. 10–12, the plots of the experimental values of P against the fiber or annual ring deviation angles are shown together with the theoretical curves estimated from Eq. 1. For the quarter- and flat-sawn boards, the transmittance periodically and widely fluctuated against the fiber deviation angle θ_f, while for the cross-cut boards the transmittance was nearly constant over the entire annual ring

deviation angle θ_a. These phenomena are theoretically the same as those for the transmission of linearly polarized visible rays through the half- and quarter-wave plates commonly used as optical elements.[6] In Figs. 11 and 12 the transmittances at 0° and 180° are smaller than those at 90° and 270°. This is because the attenuation coefficients in the fiber direction are significantly larger than those in the transverse direction (Fig. 8). Figures 11 and 12 also show that transmittances at intermediate angles are much smaller than those at the principal angles, particularly in the lower two lines. This is due to the difference between the two phase coefficients, $\Delta\beta = \beta_X - \beta_Y$, which is called birefringence.[6] This parameter is related to the difference in the propagation velocity of the electric field component of the wave between fiber and transverse directions.

Conclusions

The dielectric properties, attenuation and phase coefficients, and the transmittance were evaluated in terms of the anisotropy for hinoki (Japanese cypress) using free 100-GHz millimeter waves. The findings in this experiment were consistent with the general electromagnetic wave propagation theory for orthotropic materials.

Further examination is necessary to determine the dependency of the dielectric properties of wood on its moisture content, density, and temperature in the millimeter wave frequency range, because it has been reported that the dielectric properties depend on these properties of wood in the microwave frequency range,[13–15] and this remains a challenge to be solved at millimeter wave frequencies.

References

1. Eisele H, Haddad G (1998) Two-terminal millimeter-wave sources. IEEE Trans Microw Theory Tech 46:31–34
2. Volkov LV, Lyubchenko VE, Tikhomirov SA (1994) The arrays of GaAs antenna-coupled Schottky barrier diodes in millimeter wave imaging systems. In: Proceedings of the Gallium Arsenide Applications Symposium. GAAS®, 28–30 April 1994, Turin, pp 97–100
3. Goldsmith PF, Hsieh CT, Huguenin GR, Kapitzky J, Moore EL (1993) Focal plane imaging systems for millimeter-wavelengths. IEEE Trans Microw Theory Tech 41:1644–1675
4. Sheen DM, McMakin DD, Hall TE (2001) Three-dimensional millimeter-wave imaging for concealed weapon detection. IEEE Trans Microw Theory Tech 49:1581–1592
5. Fujii Y, Fujiwara Y, Yanase Y, Okumura S, Narahara K, Nagatsuma T, Yoshimura T, Imamura Y (2007) Nondestructive detection of termites using a millimeter-wave imaging technique. Forest Prod J 57:75–79
6. Reid M, Fedosejevs R (2006) Terahertz birefringence and attenuation properties of wood and paper. Appl Opt 45:2766–2772
7. Oyama Y, Zhen L, Tanabe T, Kagaya M (2009) Sub-terahertz imaging of defects in building blocks. NDT&E Int 42:28–33
8. Peyskens E, de Pourcq M, Stevens M, Schalck J (1984) Dielectric properties of softwood species at microwave frequencies. Wood Sci Technol 18:267–280
9. Daian G, Taube A, Birnboim A, Shramkov Y, Daian M (2005) Measuring the dielectric properties of wood at microwave frequencies. Wood Sci Technol 39:215–223
10. James WL, Yen Y-H, King RJ (1985) A microwave method for measuring moisture content, density, and grain angle of wood. USDA Research Note FPL-250, Forest Products Laboratory, Madison
11. Schajer GS, Orhan FB (2005) Microwave non-destructive testing of wood and similar orthotropic materials. Subsurf Sens Technol Appl 6:293–313
12. Torgovnikov GI (1993) Dielectric properties of wood and wood-based materials. Springer, Berlin
13. Norimoto M, Yamada T (1967) The effect of moisture content on modulus of rigidity and dielectric properties of wood. Wood Res Bull Wood Res Inst Kyoto Univ 41:36–46
14. Norimoto M, Yamada T (1969) The dielectric properties of wood II: temperature dependence of dielectric properties of wood in absolutely dried condition. Wood Res Bull Wood Res Inst Kyoto Univ 46:1–9
15. James WL (1975) Dielectric properties of wood and hardboard: variation with temperature, frequency, moisture content, and grain orientation. USDA Research Paper FPL-245, Forest Products Lavoratory, Madison